Electrical, Control and Communication Engineering

ISSN 2255-9159 (online)
2026, vol. 22, no. 1, pp. 17–30
https://doi.org/10.7250/ecce-2026-0002
Published by RTU Press

Performance Index Selection in Machinery Dynamics Instruction

Oleksandr Viktorovych Perig*
(*Associate Professor, Donbas State Engineering Academy, Kramatorsk, Ukraine*)

***Abstract* – The practical need for an effective student-centric organisation of active study by Bachelor's and Master's students of technical specialties at universities of the course on the fundamentals of optimal control theory determines the relevance of the author's methodological approach presented in this paper. The approach is associated with the development of a comprehensive individual student assignment on computational multi-criteria nonlinear optimisation modelling of various optimal controls of linear one-dimensional motion of a controlled material point within the framework of the computational visualisation of the sequential nonlinear influence of the algebraic construct of each of the minimized functionals (A1)-(A20). They were mathematically constructed from systems engineering considerations on the completely non-obvious nonlinear dynamic features of each corresponding geometric profile of the desired optimal control signal. Most of the nonlinear formulas for the minimized functionals (A3)-(A20) proposed by the author of this study are original and principally new applied scientific results for the multidisciplinary field of engineering teaching of optimal control. The calculated results of nonlinear optimisation modelling presented in this study were obtained using the computing capabilities of JModelica-{1.17; 2.14} with the Optimica extension. The study can find wide engineering and pedagogical application in teaching university disciplines in automation, cybernetic, mechanical, electromechanical, information technology and computational optimisation cycles.**

***Keywords* – Control engineering education, control nonlinearities, dynamics, key performance indicator, machine control, mechatronics, motion analysis, optimal control.**

I. Introduction

Optimal control problems with various forms of minimized functionals are of great importance in the training programs of engineering specialists in almost every technical specialty [1]–[47]. On the other hand, the vast majority of available textbooks [37]–[39] practically do not cover algorithmic, computational and software-specific features of the formulation, statement and computational solution of optimal control problems. The use of open source software [1], [4], [5] is also ignored by most available optimisation textbooks [37]–[39], which emphasizes the relevance of the presented instructional work.

Improving the teaching of optimal control theory is an important complex problem of modern engineering education, given that almost every topic of the final educational and qualification work of a candidate for higher technical education at the Bachelor's, Master's or PhD level mostly contains an ambitious formulation of a project promise regarding the successful achievement of an optimisation goal related to increasing one of such parameters of the performance of a technical process or engineering system as efficiency, productivity, quality, speed, accuracy etc.

II. Concerning CMCES Course Mapping

A freeware-enhanced introductory course of Classical Mechanics for Control Engineering Students (CMCES course) should practically acquaint freshman automation engineering major students with mechanics inspired applications of control engineering concepts and techniques in the multidisciplinary field of guided dynamics, analytical mechanics, vibration theory, mechatronics, automated control, scientific programming, engineering optimisation, and optimal control.

Generally speaking, the particle dynamics module is the standard educational component of the numerous undergraduate-, graduate- and postgradute-level courses in physics, mechanics, mechatronics, optimisation, automatic and optimal control for university students majoring in all fields and branches of modern engineering sciences [1]–[47]. Moreover, it is possible to introduce some basic concepts of automation and control engineering with a wide use of toy models of guided point dynamics within the mapped CMCES course.

The concept of control should be the central topic of the mapped CMCES course.

However, this is a complex and non-obvious didactic assignment to effectively and briefly narrate a student-friendly CMCES course, which should computationally acquaint first-year Bachelor's students majoring in automation and control engineering with mechanical illustrations of the control concept in application to guided motion description.

Today a CMCES-enhanced Optimal Control Course (OCC) should be considered as a compulsory discipline because themes of all B.Sc., M.Sc., and PhD diploma projects for the full range of engineering specialties routinely declare the standard promises of thesis, in particular, technical problem solutions through successful achievement of targeted quality criterion optimisation of technological process.

However, practically speaking, many graduate students have numerous difficulties with proper understanding of

* Corresponding author. E-mail: olexander.perig@gmail.com ; Oleksandr.Perih@ddma.edu.ua
Received 14-01-2026, accepted 02-04-2026

computational estimation and engineering interpretation of such popular quality criteria as Time-Optimal Performance Criterion (Minimum-Time Criterion) and Quadratic Quality Criterion (Quadratic Performance Index).

Moreover, undergraduate, graduate and postgraduate engineering students as well as industrially-employed graduate engineers (Dipl.-Ing.) have numerous methodological problems, associated with practical acquisition of software-implemented numerical methods and computational techniques of Optimal Control Theory (OCT).

III. The Scope of the Research

Both CMCES course-enrolled and OCC course-enrolled students should understand the difference between the different performance criteria from a practical viewpoint. It is possible to visualise the difference between different quality criteria through the application of computational possibilities of JModelica.org with Optimica extension.

The scope of this paper is focused on Modelica-enhanced student-friendly explanation of performance index-related concepts in the courses of classical mechanics, mechatronics, and optimal control.

Paper Novelty Statement: The prime scientific novelty of this study, devoted to optimal control teaching techniques, is based on the author's construction of non-obvious new algebraic forms (A3)–(A20) of minimized objective functions-functionals (A1)–(A20) that define methodologically interesting nonlinear dynamics of u-controlled one-dimensional motion of a guided material particle. Many constructs (A3)–(A20) of the Modelica-solvable nonlinear objective functions proposed by the author are fundamentally new results for freeware-assisted control engineering education.

Paper Highlights: Teaching of multicriterial optimisation in the mechanics course is provided. Original constructs of minimized functionals (A3)–(A20) are proposed. Nonlinear dynamic effects in optimal control problems are visualised.

Justification for the scientific novelty of the author's approach: In the context of verifying the statement about prime scientific novelty of the presented study, the author has thoroughly familiarised himself with the existing scientific, technical and methodological literature on engineering and engineering and pedagogical developments in the field of methodology of teaching the theory of optimal control, but has not found in previously known works [1]–[33], [35]–[47] either constructs of minimized functionals similar to the target functions (A3)–(A20) proposed by the author in Table I, or graphical plots similar to Figs. 3–20, which confirms the author's statement about the principal scientific novelty of this study.

The engineering and pedagogical implications of the presented study are consonant with the following main ideas of: I1. Systems approach in pedagogy; I2. Synergetic approach in pedagogy; I3. Cybernetic approach in pedagogy; I4. Game-based approach in pedagogy; I5. Project-based learning; I6. Constructivism in pedagogy; I7. Pragmatism in pedagogy; I8. Positivism in pedagogy; I9. Flipped classroom; I10. Finalistic approach in pedagogy; I11. Teleological approach in pedagogy; I12. Causal approach in pedagogy.

IV. Statement of a "Multi-headed" Dynamic Problem of Multi-criteria Optimal Control

Technical instructor explains to students that particle dynamics of u -controlled motion deals with two levels of particle motion description (Table I).

Lower level "B" of particle dynamics (B1)–(B6) includes Newtonian differential equations (B1) containing the phase (state) variables $\{x_1 ; x_2\}$ and control signal u, initial (B2), (B5) and boundary (B3), (B6) conditions for both phase (state) variables $\{x_1 ; x_2\}$, as well as restrictions (B3), (B6) on u-signal values, including additional restrictions on phase (state) variables $\{x_1 ; x_2\}$ etc.

Upper level "A" of particle dynamics includes the engineer-chosen structure ((A1)–(A20)) of quality criterion J (minimized functional J).

Let us consider the nature of the dynamic influence of nonlinear quality criteria ((A1)–(A20)) in the form of integral objective functions (Table I) on the one-dimensional controlled dynamics of a linearly moving point mass (Figs. 1–21). As part of the implementation of this instructional assignment, the author's set of calculation data [34], detailed Table I and the series of corresponding computational Figs. 1–21 were prepared using the computational capabilities of the open source software jModelica.org-{1.17; 2.14} with the Optimica extension [1].

Let a material point of mass $m = 1\,[\text{kg}]$ ((B4) in Table I) move rectilinearly along the horizontal Ox -axis (Fig. 21), where material particle moves sequentially from the initial $(t_0 = 0\,[\text{s}])$ phase position $\{(x(t_0)); (V(t_0))\} = \{+20\,[\text{m}]; -15\,[\text{m/s}]\}$ ((B2), (B5) in Table I; Fig. 21) to the final $(t_f = ?\,[\text{s}])$ phase position $\{(x(t_f)); (V(t_f))\} = \{-20\,[\text{m}]; -10\,[\text{m/s}]\}$ ((B3), (B6) in Table I; Fig. 21).

The control force $F(t) = u(t)\,[\text{N}]$ is applied to material point, which is the resultant of the active forces $\text{F}(t)\,[\text{N}]$, directed along Ox -axis (Fig. 21). Certain energy-power restrictions are imposed on the value of the control force $F(t) = u(t)\,[\text{N}]$: $F_{\min} \le F(t) \le F_{\max}$ or $u_{\min} \le u(t) \le u_{\max}$, where $F_{\min}(t) = u_{\min}(t)\,[\text{N}]$ and $F_{\max}(t) = u_{\max}(t)\,[\text{N}]$ are, respectively, the minimum $u_{\min}(t) = -25\,[\text{N}]$ and maximum $u_{\max}(t) = +35\,[\text{N}]$ values of the control force $F(t) = u(t)\,[\text{N}]$ ((B3), (B6) in Table I).

Using the computational capabilities of the free software JModelica.org with the Optimica extension, an engineering student was encouraged to solve twenty optimal control problems (({(A1), (B1) – (B6), Fig. 1}; … {(A20), (B1)–(B6), Fig. 20}) for one-dimensional controlled motion of material particle with achievement of minimization of the nonlinear objective functions (A1)–(A20).

For every minimized functional (A1)–(A20), the student should approximately estimate for which Modelica-optimised time interval $(t_f = ?\,[\text{s}])$ it is possible to move a material point with mass m from the initial phase position $\{x_{10}; x_{20}\}$ to the final phase position $\{x_{1f}; x_{2f}\}$, if $u_{\min} \le u(t) \le u_{\max}$ (Table I).

It is also necessary graphically visualise the corresponding functional dependencies for the control force $u = u(t) = ?\,[\mathrm{N}]$, horizontal coordinate $x_1 = x_1(t) = ?\,[\mathrm{m}]$ and particle velocity $x_2 = x_2(t) = ?\,[\mathrm{m}/s]$ on the current time *t*[s] for every particular algebraic structure among the twenty performance indices ((A1)–(A20)). The instructor draws the audience's attention to the fact that both Table I and Figs. 1–21 represent an actual example of the student's individual calculation task as part of an optimisation dynamic study of twenty possible nonlinear target functions ((A1)–(A20)).

At the initial moment of time $t = 0\,[\mathrm{s}]$, the material point was in the starting position "0", geometrically located to the right of the origin *O* with the initial Cartesian horizontal coordinate $x_{10} = +20\,[\mathrm{m}]$ and with the initial horizontal velocity $\mathbf{V_0}\,[\mathrm{m/s}]$ directed to the left $\left((\mathbf{V_0} \uparrow\downarrow x); (\mathbf{V_0} \uparrow\downarrow x_1)\right)$, with the initial direction of $\mathbf{V_0}\,[\mathrm{m/s}]$ algebraically given as $x_{20} = -15\,[\mathrm{m/s}]$, where the value of point initial velocity is $V_0 = |x_{20}| = 15\,[\mathrm{m/s}]$. The initial phase coordinates (initial coordinate; initial velocity) of the controlled material point are characterised by the numerical values of the both states $(x_{10}; x_{20}) = (+20\,[\mathrm{m}]; -15\,[\mathrm{m/s}])$, which determine the initial phase state $\{x_{10}; x_{20}\}$ of the moving material point in the state space (Fig. 21). The teacher additionally draws the students' attention to the fact that the both initial conditions $\{x_{10}; x_{20}\}$ at $t = 0\,[\mathrm{s}]$ for the one-dimensional motion of the controlled point can be visually verified by looking on the left at the zero-time values of the both calculated curves $x_1 = x_1(t)$ and $x_2 = x_2(t)$ on each of the twenty calculated graphs in Figs. 1– 20.

At the final moment of time $t = t_f\,[\mathrm{s}]$, the material point was in the final position "*f*", geometrically located to the left of the origin *O* with the final Cartesian horizontal coordinate $x_{1f} = -20\,[\mathrm{m}]$ and with the final horizontal velocity $\mathbf{V}_f\,[\mathrm{m/s}]$ directed to the left $\left((\mathbf{V}_f \uparrow\downarrow x); (\mathbf{V}_f \uparrow\downarrow x_1)\right)$, with the final direction of $\mathbf{V}_f\,[\mathrm{m/s}]$ algebraically given as $x_{2f} = -10\,[\mathrm{m/s}]$, where the value of point final velocity is $V_f = |x_{2f}| = 10\,[\mathrm{m/s}]$. The final phase coordinates (final coordinate; final velocity) of the controlled material point are characterised by the numerical values of the both terminal constraints $(x_{1f}; x_{2f}) = (-20\,[\mathrm{m}]; -10\,[\mathrm{m/s}])$, which determine the final phase state $\{x_{1f}; x_{2f}\}$ of the moving material point in the state space (Fig. 21). The teacher additionally draws the students' attention to the fact that the both final conditions (or terminal constraints) $\{x_{1f}; x_{2f}\}$ at $t = t_f\,[\mathrm{s}]$ for the one-dimensional motion of the controlled point can be visually verified by looking on the right at the final-time values of the both calculated curves $x_1 = x_1(t)$ and $x_2 = x_2(t)$ on each of the twenty calculated graphs in Figs. 1–20.

Both the initial velocity vector $\mathbf{V_0}\,[\mathrm{m/s}]$ and the final velocity vector $\mathbf{V}_f\,[\mathrm{m/s}]$ are directed to the left $\left((\mathbf{V_0} \uparrow\downarrow x); (\mathbf{V}_f \uparrow\downarrow x); (\mathbf{V_0} \uparrow\uparrow \mathbf{V}_f)\right)$ and the linear point displacement $\mathbf{0f}$ from the initial point "0" to the final point "*f*" is also directed to the left $\left((\mathbf{0f} \uparrow\downarrow x); (\mathbf{0f} \uparrow\uparrow \mathbf{V_0}); (\mathbf{0f} \uparrow\uparrow \mathbf{V}_f)\right)$. Thus, currently there are no switching in the direction of movement of the controlled point and no additional stops during particle movement occur (Fig. 21).

TABLE I

The Structure of the Following Twenty Well-Posed Optimisation Problems Proposed by the Author

A. "Head-Level" or "Upper Floor" ((A1) – (A20)) of Optimal Control Problem (Figs. 1–21): min(*J*)-Quality Criterion (Performance Index; Performance Indicator; Performance Criterion; Objective Function; Terminal Cost Function; Minimized Functional) ((A1)–(A20)):
A1. Time-Optimal Control Problem (Minimum Time Optimisation Problem): $\min\limits_{u(t)}(J_1) = \min\limits_{u(t)}(t_f);\ (\mathrm{A1})$, where {Modelica, Optimica}-optimised value $(t_f) = (t_f)_1$ of point motion final time in J_1-functional is unknown in advance $(t_f) = (t_f)_1 = ?$ (Fig. 1).
A2. Optimisation Problem with Quadratic Quality Criterion (Quadratic Performance Index) defined as integral of the sum of the squares of both phase variables and the control signal: $\min\limits_{u(t)}(J_2) = \min\limits_{u(t)}\left(\int_0^{(t_f^*)}\left(\left[(x_1(t))^2\right] + \left[(x_2(t))^2\right] + \left[(u(t))^2\right]\right)dt\right);\ (\mathrm{A2})$, where the constant upper limit of integration $(t_f^*) = ((t_f^*)_2) = const\ (s)$ has the fixed value. E.g., it was assumed in Fig. 2 that student-predetermined time of material particle motion $((t_f^*)_2) = 1.65\ (s)$ and $((t_f^*)_2) \geq ((t_f)_1)$. Therefore, the previous formula (A2) yields that $\min\limits_{u(t)}(J_2) = \min\limits_{u(t)}\left(\int_0^{1.65}\left(\left[(x_1(t))^2\right] + \left[(x_2(t))^2\right] + \left[(u(t))^2\right]\right)dt\right);\ (\mathrm{A2}^*)$.
A3. Optimisation Problem with (1/(x_i))-modified Quadratic Quality Criterion (Quadratic Performance Index) defined as integral of the sum of squares of pairwise differences of control signal and reciprocals of both phase variables: $\min\limits_{u(t)}(J_3) = \min\limits_{u(t)}\left(\int_0^{(t_f)}\left(\left(\left(\frac{1}{x_1(t)}\right) - \left(\frac{1}{x_2(t)}\right)\right)^2 + \left(\left(\frac{1}{x_1(t)}\right) - u(t)\right)^2 + \left(\left(\frac{1}{x_2(t)}\right) - u(t)\right)^2\right)dt\right);\ (\mathrm{A3})$ (Fig. 3), where {Modelica, Optimica}-optimised value $(t_f) = ((t_f)_3)$ of final time in variable upper limit of integration in minimized J_3-functional is unknown in advance $(t_f) = ((t_f)_3) = ?$
A4. Optimisation Problem with ((der(x_i))^3)-and-(u^3)-modified Integral Performance Index (Integral Quality Criterion) defined as integral of the sum of the cube of the control signal and the cubes of the first time derivatives of both phase variables:

$$\min_{u(t)}(J_4)=\min_{u(t)}\left(\int_0^{(t_f)}\left(\left[\left(\frac{d(x_1(t))}{dt}\right)^3\right]+\left[\left(\frac{d(x_2(t))}{dt}\right)^3\right]+\left[(u(t))^3\right]\right)dt\right);(\mathrm{A4})$$ (Fig. 4), where {Modelica, Optimica}-optimised value $(t_f)=((t_f)_4)$ of final time in variable upper limit of integration in minimized J_4-functional is unknown in advance $(t_f)=((t_f)_4)=?$

A5. Optimisation Problem with power (1/2)-modified Quadratic Performance Index (square root-modified Quadratic Quality Criterion) defined as integral of the square root of the sum of the squares of both phase variables and the control signal or defined as integral of the square root of the quadratic quality criterion:

$$\min_{u(t)}(J_5)=\min_{u(t)}\left(\int_0^{(t_f)}\sqrt[2]{\left(\left[(x_1(t))^2\right]+\left[(x_2(t))^2\right]+\left[(u(t))^2\right]\right)}dt\right);(\mathrm{A5})$$ (Fig. 5), where {Modelica, Optimica}-optimised value $(t_f)=((t_f)_5)$ of final time in variable upper limit of integration in minimized J_5-functional is unknown in advance $(t_f)=((t_f)_5)=?$

A6. Optimisation Problem with power (1/3)-modified Quadratic Performance Index (cube root-modified Quadratic Quality Criterion) defined as integral of the cube root of the sum of the squares of both phase variables and the control signal or defined as integral of the cube root of the quadratic quality criterion:

$$\min_{u(t)}(J_6)=\min_{u(t)}\left(\int_0^{(t_f)}\sqrt[3]{\left(\left[(x_1(t))^2\right]+\left[(x_2(t))^2\right]+\left[(u(t))^2\right]\right)}dt\right);(\mathrm{A6})$$ (Fig. 6), where {Modelica, Optimica}-optimised value $(t_f)=((t_f)_6)$ of final time in variable upper limit of integration in minimized J_6-functional is unknown in advance $(t_f)=((t_f)_6)=?$

A7. Optimisation Problem with power (1/3)-modified quadratic Performance Index (cube root-modified Quadratic Quality Criterion) defined as integral of the cube root of sum of squares of pairwise differences of both phase variables and control signal or defined as integral of the cube root of the quadratic quality criterion: $$\min_{u(t)}(J_7)=\min_{u(t)}\left(\int_0^{(t_f)}\sqrt[3]{\left((x_1(t)-x_2(t))^2+(x_1(t)-u(t))^2+(x_2(t)-u(t))^2\right)}dt\right);(\mathrm{A7})$$ (Fig. 7), where {Modelica, Optimica}-optimised value $(t_f)=((t_f)_7)$ of final time in variable upper limit of integration in minimized J_7-functional is unknown in advance $(t_f)=((t_f)_7)=?$

A8. Optimisation Problem with ($x_1 \times x_2 \times u^2$)-modified Integral Multiplicative Performance Index defined as integral of the product of the first and second phase variables multiplied by the square of the control signal or defined as integral of the product of both state variables and square of control signal:

$$\min_{u(t)}(J_8)=\min_{u(t)}\left(\int_0^{(t_f)}\left((x_1(t))\cdot(x_2(t))\cdot\left[(u(t))^2\right]\right)dt\right);(\mathrm{A8})$$ (Fig. 8), where {Modelica, Optimica}-optimised value $(t_f)=((t_f)_8)$ of final time in variable upper limit of integration in minimized J_8-functional is unknown in advance $(t_f)=((t_f)_8)=?$

A9. Optimisation Problem with $((\mathrm{d}(x_1)/\mathrm{d}t)\times(\mathrm{d}(x_2)/\mathrm{d}t))\times u$-modified Integral Multiplicative Performance Index defined as integral of the product of the control signal and the first time derivative of the first phase variable, multiplied by the first time derivative of the second phase variable, or defined as integral of the product of time-rates of both state variables and control signal:

$$\min_{u(t)}(J_9)=\min_{u(t)}\left(\int_0^{(t_f)}\left(\left[\left(\frac{d(x_1(t))}{dt}\right)\right]\cdot\left[\left(\frac{d(x_2(t))}{dt}\right)\right]\cdot(u(t))\right)dt\right);(\mathrm{A9})$$ (Fig. 9), where Optimica-optimised value $(t_f)=((t_f)_9)$ of final time in variable upper limit of integration in minimized J_9-functional is unknown in advance $(t_f)=((t_f)_9)=?$

A10. Optimisation Problem with $(((x_i)^1-u)^1\times(\mathrm{d}(x_i)/\mathrm{d}t)^1)$-modified Integral Multiplicative Performance Index defined as integral of the product of the first time derivative of the first phase variable and the first time derivative of the second phase variable, multiplied by the difference between the first phase variable and the control signal, and also multiplied by the difference between the second phase variable and the control signal:

$$\min_{u(t)}(J_{10})=\min_{u(t)}\left(\int_0^{(t_f)}\left(((x_1(t))-u(t))\cdot((x_2(t))-u(t))\cdot\left(\frac{d(x_1(t))}{dt}\right)\cdot\left(\frac{d(x_2(t))}{dt}\right)\right)dt\right);(\mathrm{A10})$$ (Fig. 10), where Optimica-optimised value $(t_f)=((t_f)_{10})$ of final time in variable upper limit of integration in minimized J_{10}-functional is unknown in advance $(t_f)=((t_f)_{10})=?$

A11. Optimisation Problem with $(((x_i)^2-\mathrm{u})^2\times((\mathrm{d}(x_i)/\mathrm{d}t)^2-u))$-modified Integral Multiplicative Performance Index defined as integral of the product of the difference of the square of the first time derivative of the first phase variable minus the control signal, multiplied by the difference of the square of the first time derivative of the second phase variable minus the control signal, multiplied by the square of the difference of the square of the first phase variable minus the control signal, and also multiplied by the square of the difference of the square of the second phase variable minus the control signal:

$$\min_{u(t)}(J_{11})=\min_{u(t)}\left(\int_0^{(t_f)}\left(\left(\left((x_1(t))^2-u(t)\right)^2\right)\cdot\left(\left((x_2(t))^2-u(t)\right)^2\right)\cdot\left(\left(\frac{d(x_1(t))}{dt}\right)^2-u(t)\right)\cdot\left(\left(\frac{d(x_2(t))}{dt}\right)^2-u(t)\right)\right)dt\right);\ (\mathrm{A11})$$ (Fig. 11), where optimised value $(t_f)=((t_f)_{11})$ of final time in variable upper limit of integration in minimized J_{11}-functional is unknown in advance $(t_f)=((t_f)_{11})=?$

A12. Optimisation Problem with $(((x_i)^2 - u)^2\times((d(x_i)/dt)^2 + u))$-modified Integral Multiplicative Performance Index defined as integral of the product of the sum of the square of the first time derivative of the first phase variable with the addition of the control signal, multiplied by the sum of the square of the first time derivative of the second phase variable with the addition of the control signal, multiplied by the square of the difference of the square of the first phase variable minus the control signal, and also multiplied by the square of the difference of the square of the second phase variable minus the control signal:

$$\min_{u(t)}(J_{12})=\min_{u(t)}\left(\int_0^{(t_f)}\left(\left(\left((x_1(t))^2-u(t)\right)^2\right)\cdot\left(\left((x_2(t))^2-u(t)\right)^2\right)\cdot\left(\left(\frac{d(x_1(t))}{dt}\right)^2+u(t)\right)\cdot\left(\left(\frac{d(x_2(t))}{dt}\right)^2+u(t)\right)\right)dt\right);\ (\mathrm{A12})$$ (Fig. 12), where optimised value $(t_f)=((t_f)_{12})$ of final time in variable upper limit of integration in minimized J_{12}-functional is unknown in advance $(t_f)=((t_f)_{12})=?$

A13. Optimisation Problem with $((x_1)^2\times(x_2)^2\times u^2)$-modified Integral Multiplicative Performance Index defined as integral of the product of the square of the first and square of the second phase variables multiplied by the square of the control signal or defined as integral of the product of the squares of state variables and control signal: $$\min_{u(t)}(J_{13})=\min_{u(t)}\left(\int_0^{(t_f)}\left(\left[(x_1(t))^2\right]\cdot\left[(x_2(t))^2\right]\cdot\left[(u(t))^2\right]\right)dt\right);\ (\mathrm{A13})$$ (Fig. 13), where {Modelica, Optimica}-optimised value $(t_f)=((t_f)_{13})$ of final time in variable upper limit of integration in minimized J_{13}-functional is unknown in advance $(t_f)=((t_f)_{13})=?$

A14. Optimisation Problem with $(((x_i)^2 + u)^2\times((d(x_i)/dt)^2 + u))$-modified Integral Multiplicative Performance Index defined as integral of the product of the sum of the square of the first time derivative of the first phase variable with the addition of the control signal, multiplied by the sum of the square of the first time derivative of the second phase variable with the addition of the control signal, multiplied by the square of the sum of the square of the first phase variable with the addition of the control signal, and also multiplied by the square of the sum of the square of the second phase variable with the addition of the control signal:

$$\min_{u(t)}(J_{14})=\min_{u(t)}\left(\int_0^{(t_f)}\left(\left(\left((x_1(t))^2+u(t)\right)^2\right)\cdot\left(\left((x_2(t))^2+u(t)\right)^2\right)\cdot\left(\left(\frac{d(x_1(t))}{dt}\right)^2+u(t)\right)\cdot\left(\left(\frac{d(x_2(t))}{dt}\right)^2+u(t)\right)\right)dt\right);\ (\mathrm{A14})$$ (Fig. 14), where optimised value $(t_f)=((t_f)_{14})$ of final time in variable upper limit of integration in minimized J_{14}-functional is unknown in advance $(t_f)=((t_f)_{14})=?$

A15. Optimisation Problem with $(((x_i)^3 - u)^1\times(d(x_i)/dt)^3)$-modified Integral Multiplicative Performance Index defined as integral of the product of the cube of the first time derivative of the first phase variable and the cube of the first time derivative of the second phase variable, multiplied by the difference of the cube of the first phase variable minus the control signal, and also multiplied by the difference of the cube of the second phase variable minus the control signal:

$$\min_{u(t)}(J_{15})=\min_{u(t)}\left(\int_0^{(t_f)}\left(\left((x_1(t))^3-u(t)\right)\cdot\left((x_2(t))^3-u(t)\right)\cdot\left(\left(\frac{d(x_1(t))}{dt}\right)^3\right)\cdot\left(\left(\frac{d(x_2(t))}{dt}\right)^3\right)\right)dt\right);\ (\mathrm{A15})$$ (Fig. 15), where Optimica-optimised value $(t_f)=((t_f)_{15})$ of final time in variable upper limit of integration in minimized J_{15}-functional is unknown in advance $(t_f)=((t_f)_{15})=?$

A16. Optimisation Problem with $(((x_i)^3 + u)^1\times(d(x_i)/dt)^3)$-modified Integral Multiplicative Performance Index defined as integral of the product of the cube of the first time derivative of the first phase variable and the cube of the first time derivative of the second phase variable, multiplied by the sum of the cube of the first phase variable with the addition of the control signal, and also multiplied by the sum of the cube of the second phase variable with the addition of the control signal: $$\min_{u(t)}(J_{16})=\min_{u(t)}\left(\int_0^{(t_f)}\left(\left((x_1(t))^3+u(t)\right)\cdot\left((x_2(t))^3+u(t)\right)\cdot\left(\left(\frac{d(x_1(t))}{dt}\right)^3\right)\cdot\left(\left(\frac{d(x_2(t))}{dt}\right)^3\right)\right)dt\right);\ (\mathrm{A16})$$ (Fig. 16), where Optimica-optimised value $(t_f)=((t_f)_{16})$ of final time in variable upper limit of integration in minimized J_{16}-functional is unknown in advance $(t_f)=((t_f)_{16})=?$

A17. Optimisation Problem with $(((x_i)^3 - u^2)^1\times((d(x_i)/dt)^3 - u^2))$-modified Integral Multiplicative Performance Index defined as integral of the product of the difference of the cube of the first time derivative of the first phase variable minus the square of the control signal, multiplied by the difference of the cube of the first time derivative of the second phase variable minus the square of the control signal, multiplied by the difference of the cube of the first phase variable minus the square of the control signal, multiplied by the difference of the cube of the second phase variable minus the square of the control signal (Fig. 17):

$$\min_{u(t)}(J_{17})=\min_{u(t)}\left(\int_0^{(t_f)}\left(\left((x_1(t))^3-(u(t))^2\right)\cdot\left((x_2(t))^3-(u(t))^2\right)\cdot\left(\left(\frac{d(x_1(t))}{dt}\right)^3-(u(t))^2\right)\cdot\left(\left(\frac{d(x_2(t))}{dt}\right)^3-(u(t))^2\right)\right)dt\right);\ (\mathrm{A17}),$$ where optimised value $(t_f)=((t_f)_{17})$ of final time in variable upper limit of integration in minimized J_{17}-functional is unknown in advance $(t_f)=((t_f)_{17})=?$

A18. Optimisation Problem with $(((x_i)^3 + u^2)^1\times((d(x_i)/dt)^3 + u^2))$-modified Integral Multiplicative Performance Index defined as integral of the product of the sum of the cube of the first time derivative of the first phase variable with the addition of the square of the control signal, multiplied by the sum of the cube of the first time derivative of the second phase variable with the addition of the square of the control signal, multiplied by the sum of the cube of the first phase variable with the addition of the square of the control signal, multiplied by the sum of the cube of the second phase variable with the addition of the square of

the control signal (Fig. 18): $\min_{u(t)}(J_{18})=\min_{u(t)}\left(\int_0^{(t_f)}\left(((x_1(t))^3+(u(t))^2)\cdot((x_2(t))^3+(u(t))^2)\cdot\left(\left(\frac{d(x_1(t))}{dt}\right)^3+(u(t))^2\right)\cdot\left(\left(\frac{d(x_2(t))}{dt}\right)^3+(u(t))^2\right)\right)dt\right)$; (A18), where optimised value $(t_f)=((t_f)_{18})$ of final time in variable upper limit of integration in minimized J_{18}-functional is unknown in advance $(t_f)=((t_f)_{18})=?$		
A19. Optimisation Problem with $(((x_i)^4-u)^1\times(d(x_i)/dt)^4)$-modified Integral Multiplicative Performance Index defined as integral of the product of the fourth power of the first time derivative of the first phase variable, multiplied by the fourth power of the first time derivative of the second phase variable, multiplied by the difference of the fourth power of the first phase variable minus the control signal, and also multiplied by the difference of the fourth power of the second phase variable minus the control signal: $\min_{u(t)}(J_{19})=\min_{u(t)}\left(\int_0^{(t_f)}\left(((x_1(t))^4-u(t))\cdot((x_2(t))^4-u(t))\cdot\left(\left(\frac{d(x_1(t))}{dt}\right)^4\right)\cdot\left(\left(\frac{d(x_2(t))}{dt}\right)^4\right)\right)dt\right)$; (A19) (Fig. 19), where optimised value $(t_f)=((t_f)_{19})$ of final time in variable upper limit of integration in minimized J_{19}-functional is unknown in advance $(t_f)=((t_f)_{19})=?$		
A20. Optimisation Problem with $(\exp((-1)\times x_1))\times(\sin((u-1)^2))$-modified Integral Multiplicative Performance Index defined as integral of the product of the sine of the square of the difference in the control signal minus one, multiplied by the number e raised to the power of the negative value of the first phase variable: $\min_{u(t)}(J_{20})=\min_{u(t)}\left(\int_0^{(t_f)}\left[\sin((u(t)-1)^2)\right]\cdot\left[\exp(-x_1(t))\right]dt\right)$; (A20) (Fig. 20), where {Modelica, Optimica}-optimised value $(t_f)=((t_f)_{20})$ of final time in variable upper limit of integration in minimized J_{20}-functional is unknown in advance $(t_f)=((t_f)_{20})=?$		
B. “Torso-Level” or “Ground Floor” ((B1) – (B6)) of Optimal Control Problem (Figs. 1–21):		
B1. Newtonian Dynamic System {Dynamic Equations}	B2. Initial (Start) Conditions {The States}	B3. Terminal (Final) Conditions {The Constraints}
$\begin{cases}\left(\frac{d(x_1(t))}{dt}\right)=(x_2(t));\\ \left(\frac{d(x_2(t))}{dt}\right)=\left(\frac{u(t)}{\mathrm{m}}\right);\end{cases}$ (B1)	$\begin{cases}x_1(0)=x_{10};\\ x_2(0)=x_{20};\end{cases}$ (B2)	$\begin{cases}x_1(t_f)=x_{1f};\\ x_2(t_f)=x_{2f};\\ u_{\min}\le u(t)\le u_{\max};\end{cases}$ (B3)
B4. Numerical Values (B4)–(B6) for Optimisation Problem (B1)–(B3) Parameters:		
$\mathrm{m}=1\,[\mathrm{kg}]$; (B4) (Figs. 1 – 21)	$\begin{cases}x_{10}=+20\,[\mathrm{m}];\\ x_{20}=-15\,[\mathrm{m/s}];\end{cases}$ (B5)	$\begin{cases}x_{1f}=-20\,[\mathrm{m}];\\ x_{2f}=-10\,[\mathrm{m/s}];\\ -25\,[\mathrm{N}]\le u(t)\le +35\,[\mathrm{N}].\end{cases}$ (B6)

Kinematic schematic for the numerical values of the $\{x_{10};x_{20}\}$-states (B2), (B5) and the $\{x_{1f};x_{2f}\}$-constraints (B3), (B6) in computational Figs. 1–20 is shown in Fig. 21.

Performance index-dependent Modelica-derived solutions of optimal control problems ((A1)–(A20)) were numerically computed for one and the same boundary value problem (B1)–(B3) of Newtonian dynamics for material point linear motion from right to left without additional stop-points but with different structures (Table I) of minimized J-functionals in Figs. 1–20 [34].

Fig. 1 shows the numerical solution of time-optimal $\min(J_1)$-optimisation problem {(A1), (B1) – (B6)} with Modelica-optimised minimum time $(t_f)=((t_f)_1)\approx 1.63\,(s)$ of particle motion.

Fig. 1 shows the “model” graphs of the solution of the problem of optimal speed of response, from which it is evident that the controlled material point at the initial moment of time $(t_0)=0\,[\mathrm{s}]$ leaves the initial phase position “0” with the initial phase coordinates $(x_{10};x_{20})=(+20\,[\mathrm{m}];-15\,[\mathrm{m/s}])$ and during some previously unknown shortest time t_{f1} moves to the final phase position “f” with the final phase coordinates $(x_{1f};x_{2f})=(-20\,[\mathrm{m}];-10\,[\mathrm{m/s}])$ without any additional stops in the process of movement, and in this case all three vectors $\mathbf{0f}$; $\mathbf{V_0}$ and $\mathbf{V}_f$ are directed to the left, i.e., are collinear and co-directed with respect to each other: $((\mathbf{0f}\uparrow\uparrow\mathbf{V_0});(\mathbf{0f}\uparrow\uparrow\mathbf{V}_f);(\mathbf{V_0}\uparrow\uparrow\mathbf{V}_f))$.

It is useful to compare all $\min(J_i)$-dependent $(\{x_1,x_2,u\}_i)$-plots in Modelica-derived Figs. 2–20 with Fig. 1 – outlined $(\{x_1,x_2,u\}_1)$– plots assuming consideration of (A1) criterion-associated Fig. 1 as a comparator.

Fig. 2 shows that quadratic quality criterion {(A2), (B1) – (B6)} yields Fig. 1 – similar plots for predetermined $((t_f^*)_2)$ – final-time moments $((t_f^*)_2)\le((t_f)_1)$ and $((t_f^*)_2)\approx((t_f)_1)+\varepsilon$.

In this case, the calculated Fig. 2 shows the effect of parabolic smoothing of the minimum break in the linear velocity x_2 of the moving material point in Fig. 1.

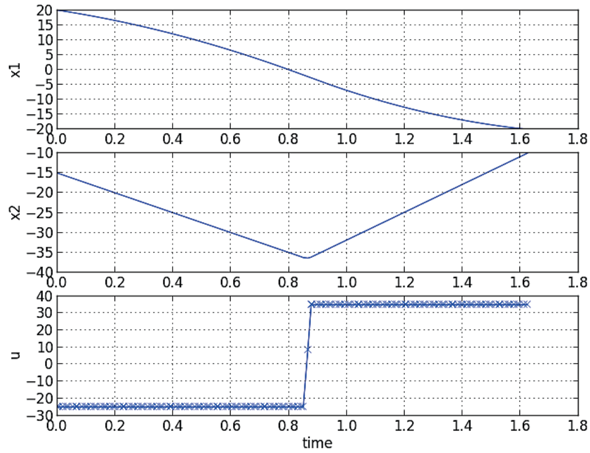

Fig. 1. Modelica-derived numerical bang-bang solution of the time-optimal control problem {(A1), (B1)–(B6)} for the one-dimensional horizontal motion of the guided point mass from initial to final phase position in the case of the (A1)-quality criterion minimization with minimum motion time achievement, where Optimica-optimised value $(t_f)=((t_f)_1)$ of point motion final time in variable upper limit of integration in minimized (A1)-functional is unknown in advance $((t_f)_1)=?$ and the value of $(t_f)=((t_f)_1)=((t_f)_{(J1)})\approx 1.63\,(s)$ was estimated in Fig. 1.

While studying the numerical methods course, students may have heard terms such as "quadratic smoothing" or "quadratic parabola smoothing" (Fig. 2).

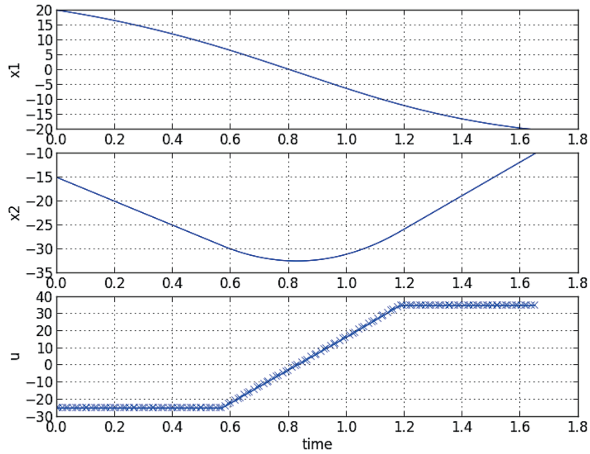

Fig. 2. Modelica-derived numerical solution of the optimal control problem {(A2), (B1)–(B6)} for the one-dimensional horizontal motion of the guided point mass in the case of the (A2, A2*)-quadratic quality criterion minimization where (A2*) has the form of the defined integral with the constant upper limit of integration $(t_f^*)=((t_f^*)_{J2})=((t_f^*)_2)=1.65\,(s)$, where the particular numerical value of the predetermined time of material particle motion $((t_f^*)_2)$ in (A2*) was chosen as $((t_f^*)_2)\approx((t_f)_1)+\varepsilon$ based on the visually observed parabolic smoothing of the minimum break of x_2- velocity curve in Fig. 1, plotted for the case A1.

At the same time, a visual comparison of the "middle" x_2-graphs in the calculated Fig. 1 and Fig. 2 clearly shows students what "quadratic smoothing" (Fig. 2) of the lower break of the linear velocity (Fig. 1) looks like in practice within the framework of using the computational capabilities of the quadratic quality criterion (A2).

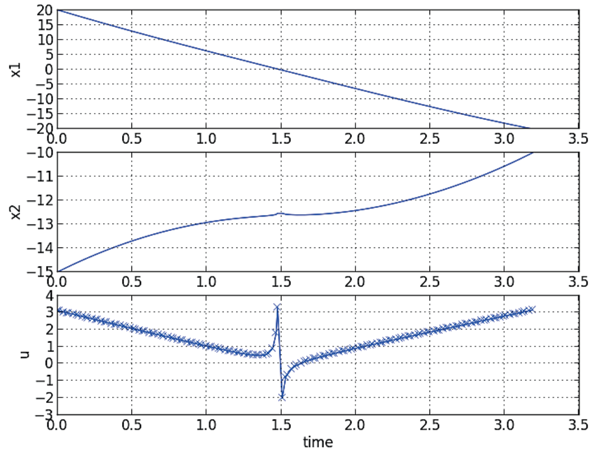

Fig. 3. Solution of the $(1/(x_i))$-modified optimal control problem {(A3), (B1)–(B6)} for the one-dimensional horizontal motion of the guided point mass from initial to final phase position in the case of the (A3)-modified quadratic quality criterion minimization where Optimica-optimised value $(t_f)=((t_f)_3)$ of point motion final time in variable upper limit of integration in $(1/(x_i))$-modified minimized quadratic (A3)-functional is unknown in advance $((t_f)_3)=?$ and the numerical value of $(t_f)=((t_f)_3)=((t_f)_{(J3)})\approx 3.2\,(s)$ was estimated according to computational plots in Fig. 3, and where time $((t_f)_3)>((t_f)_1)$.

Figs. 1, 9, 15–18 show almost the same values of Modelica-optimised final times.

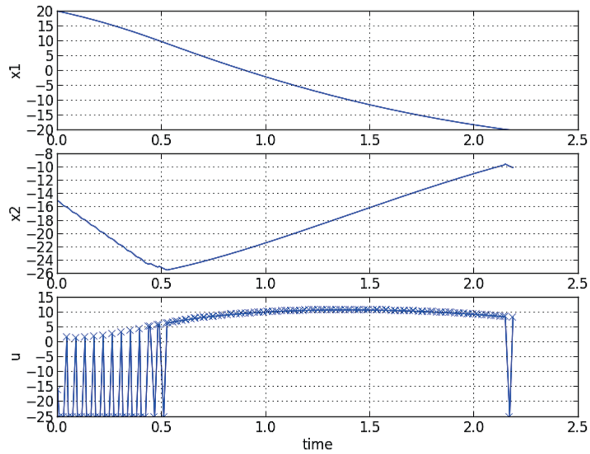

Fig. 4. Solution of the $((\mathrm{der}(x_i))^3)$-and-(u^3)-modified optimal control problem {(A4), (B1)–(B6)} for the one-dimensional horizontal motion of the guided point mass from initial to final phase position in the case of the (A4)-modified quality criterion minimization where Optimica-optimised value $(t_f)=((t_f)_4)$ of point motion final time in variable upper limit of integration in $((\mathrm{der}(x_i))^3)$-and-(u^3)-modified minimized (A4)-functional is unknown in advance and the numerical value of $(t_f)=((t_f)_4)=((t_f)_{(J4)})\approx 2.15\,(s)$ was estimated according to plots in Fig. 4, and where point motion time $((t_f)_4)>((t_f)_1)$.

Comparison of the lower u-graphs in the calculated Fig. 1 and Fig. 3 allows us to compare the nature of switching of the u-control signal depending on the use of the nonlinear target function A1 (Fig. 1) or A3 (Fig. 3).

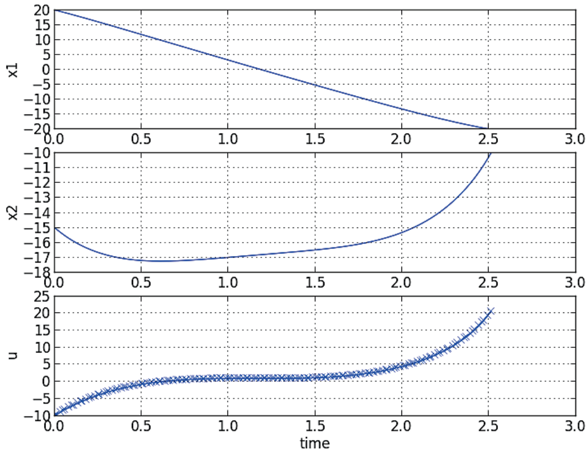

Fig. 5. Solution of the power (1/2)-modified optimal control problem {(A5), (B1)–(B6)} for the one-dimensional horizontal motion of the guided point mass from initial to final phase position in the case of the (A5)-modified quadratic quality criterion minimization where Optimica-optimised value of point motion final time in variable upper limit of integration in power (1/2)-modified minimized quadratic (A5)-functional is unknown in advance and the numerical value of $\left(t_f\right)=\left(\left(t_f\right)_5\right)=\left(\left(t_f\right)_{(J5)}\right)\approx 2.52\,(s)$ was approximately estimated according to computational plots in Fig. 5, and where point motion time $\left(\left(t_f\right)_5\right)>\left(\left(t_f\right)_1\right)$.

Figs. 4, 8–10 show only initial oscillations of $u(t)$-signal.

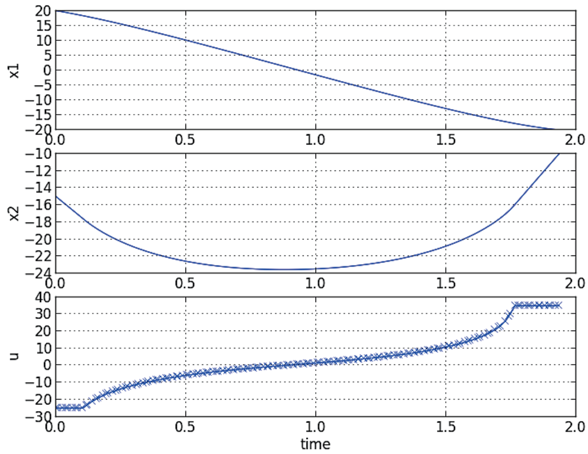

Fig. 6. Solution of the power (1/3)-modified optimal control problem {(A6), (B1)–(B6)} for the one-dimensional horizontal motion of the guided point mass from initial to final phase position in the case of the (A6)-modified quadratic quality criterion minimization where Optimica-optimised value $\left(t_f\right)=\left(\left(t_f\right)_6\right)$ of point motion final time in variable upper limit of integration in power (1/3)-modified minimized quadratic (A6)-functional is unknown in advance and the numerical value of $\left(t_f\right)=\left(\left(t_f\right)_6\right)=\left(\left(t_f\right)_{(J6)}\right)\approx 1.9\,(s)$ was estimated according to plots in Fig. 6, and where point motion time $\left(\left(t_f\right)_6\right)>\left(\left(t_f\right)_1\right)$.

The jump-like switching of the u-control signal in Fig. 1 from the minimum value $u_{\min}$ to the maximum value $u_{\max}$ occurs in the form of a u-step rising from left to right with horizontal bases. The jump-like switching of the u-control signal in Fig. 3 from the maximum value $u^*_{\max}$ to the minimum value $u^*_{\min}$ occurs in the form of a u-step descending from left to right with hyperbolic bases.

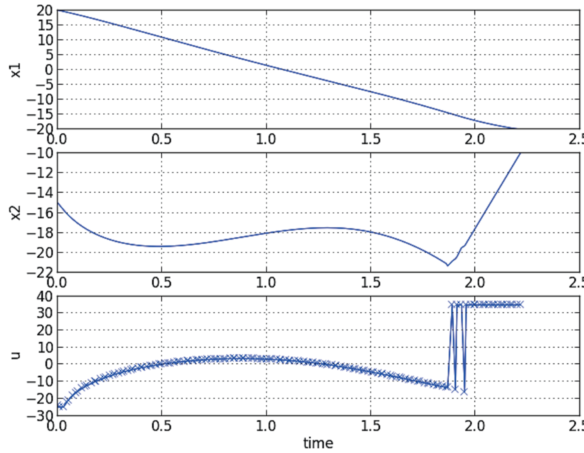

Fig. 7. Solution of the power (1/3)-modified optimal control problem {(A7), (B1)–(B6)} for the one-dimensional horizontal motion of the guided point mass from initial to final phase position in the case of the (A7)-modified quadratic quality criterion minimization where Optimica-optimised value of point motion final time in variable upper limit of integration in power (1/3)-modified minimized quadratic (A7)-functional is unknown in advance and the numerical value of $\left(t_f\right)=\left(\left(t_f\right)_7\right)=\left(\left(t_f\right)_{(J7)}\right)\approx 2.2\,(s)$ was approximately estimated according to computational plots in Fig. 7, and where point motion time $\left(\left(t_f\right)_7\right)>\left(\left(t_f\right)_1\right)$.

Figs. 9–12, 15–19 show rather central oscillations of $u(t)$-signal.

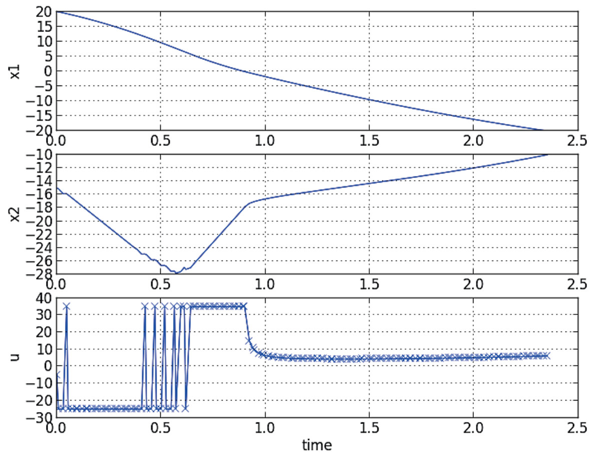

Fig. 8. Solution of the $(x_1{\times}x_2{\times}u^2)$-modified optimal control problem {(A8), (B1)–(B6)} for the 1D horizontal motion of the guided point mass from initial to final phase position in the case of the (A8)-modified multiplicative quality criterion minimization where Optimica-optimised value $\left(t_f\right)=\left(\left(t_f\right)_8\right)$ of point motion final time in variable upper limit of integration in $(x_1{\times}x_2{\times}u^2)$-modified minimized (A8)-functional is unknown in advance $\left(\left(t_f\right)_8\right)=?$ and the numerical value of $\left(t_f\right)=\left(\left(t_f\right)_8\right)=\left(\left(t_f\right)_{(J8)}\right)\approx 2.35\,(s)$ was estimated according to plots in Fig. 8, and where point motion time $\left(\left(t_f\right)_8\right)>\left(\left(t_f\right)_1\right)$.

It is important to note that Figs. 1, 9, 15–18 visualise practically very similar trends in the controlled motion of a material point with close values of the motion time

$t_{fI}^{*} \approx 1.65$ [s] in Figs. 1, 9; $t_{fII}^{*} \approx 1.7$ [s] in Figs. 16, 18; $t_{fIII}^{*} \approx 1.75$ [s] in Fig. 15 and $t_{fIV}^{*} \approx 1.78$ [s] in Fig. 17.

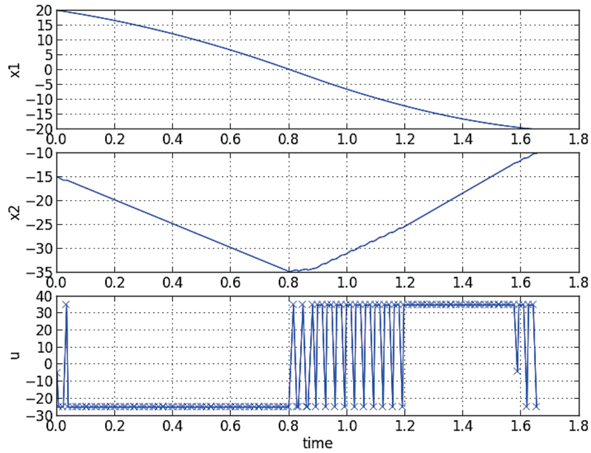

Fig. 9. Solution of the $((\mathrm{d}(x_1)/\mathrm{d}t)\times(\mathrm{d}(x_2)/\mathrm{d}t))\times u$-modified optimal control problem {(A9), (B1)–(B6)} for the 1D horizontal motion of the guided point mass from initial to final phase position in the case of the (A9)-modified multiplicative quality criterion minimization where optimised value $(t_f) = ((t_f)_9)$ of point motion final time in variable upper limit of integration in $((\mathrm{d}(x_1)/\mathrm{d}t)\times(\mathrm{d}(x_2)/\mathrm{d}t))\times u$-modified minimized (A9)-functional is unknown in advance $((t_f)_9) = ?$ and the numerical value of $(t_f) = ((t_f)_9) = ((t_f)_{(J9)}) \approx 1.67\ (s)$ was estimated according to plots in Fig. 9, and where point motion time $((t_f)_9) \geq ((t_f)_1)$.

Figs. 9 and 10 show both initial and central oscillations of $u(t)$-signal.

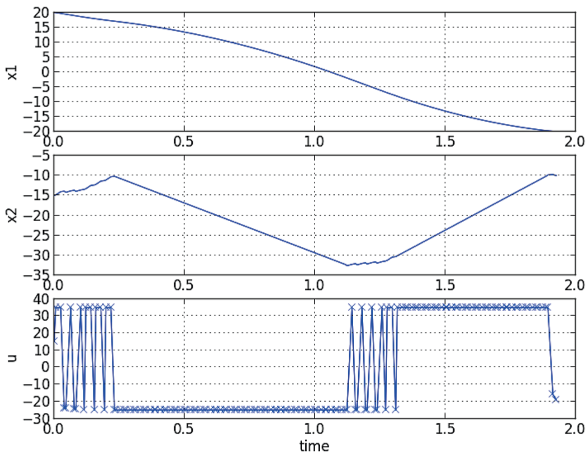

Fig. 10. Solution of the $(((x_i)^1 - u)^1\times(\mathrm{d}(x_i)/\mathrm{d}t)^1)$-modified optimal control problem {(A10), (B1)–(B6)} for the 1D horizontal motion of the guided point mass from initial to final phase position in the case of the (A10)-modified multiplicative quality criterion minimization where optimised value $(t_f) = ((t_f)_{10})$ of point motion final time in variable upper limit of integration in $(((x_i)^1 - u)^1\times(\mathrm{d}(x_i)/\mathrm{d}t)^1)$-modified minimized (A10)-functional is unknown in advance $((t_f)_{10}) = ?$ and the value of $(t_f) = ((t_f)_{10}) = ((t_f)_{(J10)}) \approx 1.9\ (s)$ was estimated according to plots in Fig. 10, and where point motion time $((t_f)_{10}) > ((t_f)_1)$.

All the “middle” x_2-graphs in Figs. 1, 9, 15–18 “tend to reproduce” the same “V”-like shape of the piecewise linear velocity graph (Figs. 1, 9), and the x_2-graphs in Figs. 15–18 approximate the degree of the lower inflection rather in the form of a “W”-like shape.

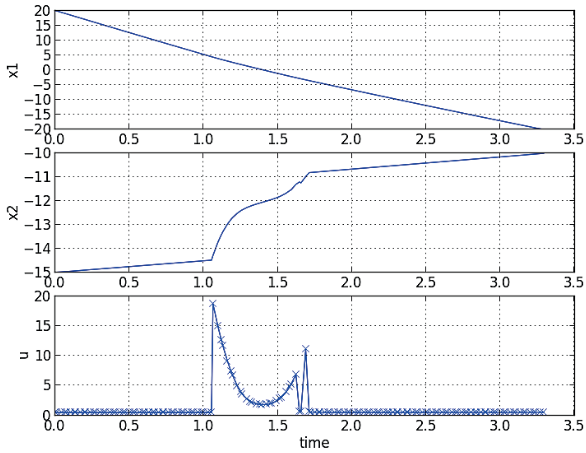

Fig. 11. Solution of the $(((x_i)^2 - u)^2\times((\mathrm{d}(x_i)/\mathrm{d}t)^2 - u))$-modified optimal control problem {(A11), (B1)–(B6)} for the 1D horizontal motion of the guided point mass from initial to final phase position in the case of the (A11)-modified multiplicative quality criterion minimization where optimised value $(t_f) = ((t_f)_{11})$ of point motion final time in variable upper limit of integration in $(((x_i)^2 - u)^2\times((\mathrm{d}(x_i)/\mathrm{d}t)^2 - u))$-modified minimized (A11)-functional is unknown in advance $((t_f)_{11}) = ?$ and the numerical value of $(t_f) = ((t_f)_{11}) = ((t_f)_{(J11)}) \approx 3.3\ (s)$ was estimated according to plots in Fig. 11, and where point motion time $((t_f)_{11}) > ((t_f)_1)$.

Figs. 7, 20 show rather final oscillations of $u(t)$-signal.

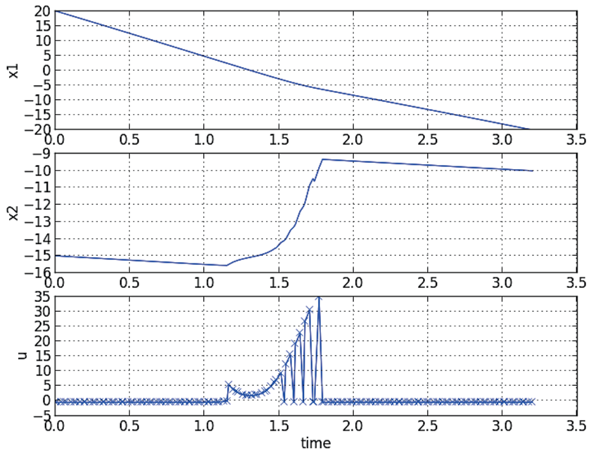

Fig. 12. Solution of the $(((x_i)^2 - u)^2\times((\mathrm{d}(x_i)/\mathrm{d}t)^2 + u))$-modified optimal control problem {(A12), (B1)–(B6)} for the 1D horizontal motion of the guided point mass from initial to final phase position in the case of the (A12)-modified multiplicative quality criterion minimization where optimised value $(t_f) = ((t_f)_{12})$ of point motion final time in variable upper limit of integration in $(((x_i)^2 - u)^2\times((\mathrm{d}(x_i)/\mathrm{d}t)^2 + u))$-modified minimized (A12)-functional is unknown in advance $((t_f)_{12}) = ?$ and the numerical value of $(t_f) = ((t_f)_{12}) = ((t_f)_{(J12)}) \approx 3.3\ (s)$ was estimated according to plots in Fig. 12, and where point motion time $((t_f)_{12}) > ((t_f)_1)$.

All u-graphs in Figs. 1, 9, 15–18 "tend to reproduce" the same shape of the "rising" step of the control signal (Figs. 1, 9), and the u-graphs in Figs. 15–18 approximate the shape of the "ascending" step in the form of two successively increasing steps, but with a lower "pit" between them.

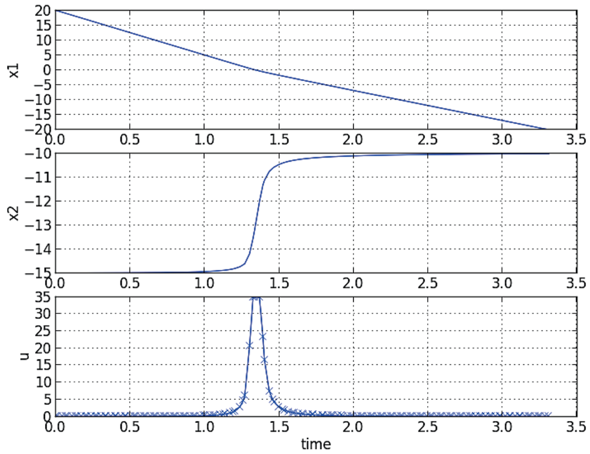

Fig. 13. Solution of the $((x_1)^2{\times}(x_2)^2{\times}u^2)$-modified optimal control problem {(A13), (B1)–(B6)} for the 1D horizontal motion of the guided point mass from initial to final phase position in the case of the (A13)-modified multiplicative quality criterion minimization where Optimica-optimised value $(t_f) = ((t_f)_{13})$ of point motion final time in variable upper limit of integration in $((x_1)^2{\times}(x_2)^2{\times}u^2)$-modified minimized (A13)-functional is unknown in advance $((t_f)_{13}) = ?$ and the numerical value of $(t_f) = ((t_f)_{13}) = ((t_f)_{(J13)}) \approx 3.35\,(s)$ was estimated according to plots in Fig. 13, and where point motion time $((t_f)_{13}) > ((t_f)_1)$.

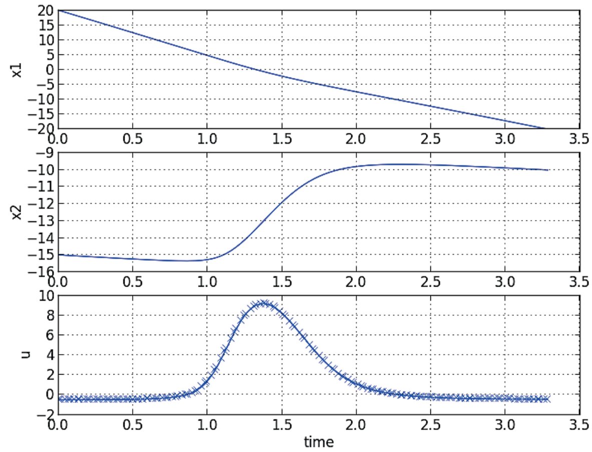

Fig. 14. Solution of the $(((x_i)^2 + u)^2{\times}((\mathrm{d}(x_i)/\mathrm{d}t)^2 + u))$-modified optimal control problem {(A14), (B1)–(B6)} for the 1D horizontal motion of the guided point mass from initial to final phase position in the case of the (A14)-modified multiplicative quality criterion minimization where optimised value $(t_f) = ((t_f)_{14})$ of point motion final time in variable upper limit of integration in $(((x_i)^2 + u)^2{\times}((\mathrm{d}(x_i)/\mathrm{d}t)^2 + u))$-modified minimized (A14)-functional is unknown in advance $((t_f)_{14}) = ?$ and the numerical value of $(t_f) = ((t_f)_{14}) = ((t_f)_{(J14)}) \approx 3.3\,(s)$ was estimated according to plots in Fig. 14, and where point motion time $((t_f)_{14}) > ((t_f)_1)$.

More complex geometrically nonlinear forms of two "sequentially rising" curved-curvilinear "ascending" steps of the u-control signal in Figs. 15–18 obviously influence the nature of the lower breaks of the x_2-velocity graph, transforming the "V"-shaped form of velocity profile in Figs. 1, 9 into the "W"-shaped form of velocity in Figs. 15–18.

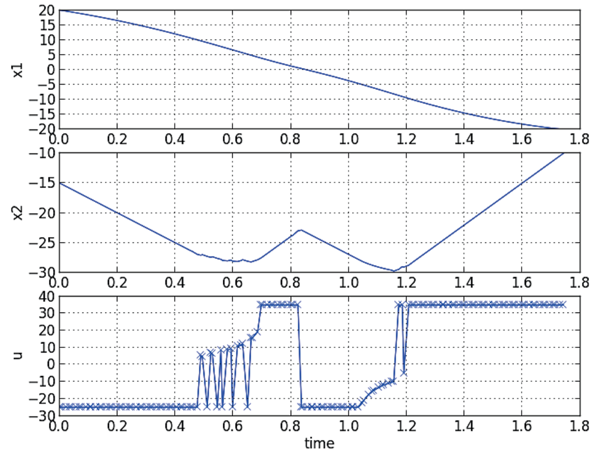

Fig. 15. Solution of the $(((x_i)^3 - u)^1{\times}(\mathrm{d}(x_i)/\mathrm{d}t)^3)$-modified optimal control problem {(A15), (B1)–(B6)} for the 1D horizontal motion of the guided point mass from initial to final phase position in the case of the (A15)-modified multiplicative quality criterion minimization where optimised value $(t_f) = ((t_f)_{15})$ of point motion final time in variable upper limit of integration in $(((x_i)^3 - u)^1{\times}(\mathrm{d}(x_i)/\mathrm{d}t)^3)$-modified minimized (A15)-functional is unknown in advance $((t_f)_{15}) = ?$ and the numerical value of $(t_f) = ((t_f)_{15}) = ((t_f)_{(J15)}) \approx 1.75\,(s)$ was estimated according to plots in Fig. 15, and where point motion time $((t_f)_{15}) \geq ((t_f)_1)$.

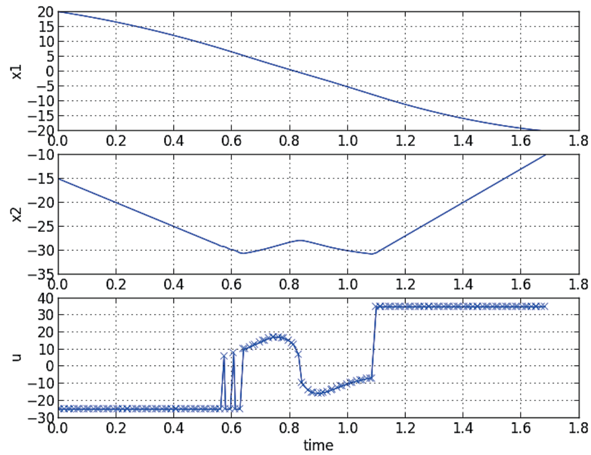

Fig. 16. Solution of the $(((x_i)^3 + u)^1{\times}(\mathrm{d}(x_i)/\mathrm{d}t)^3)$-modified optimal control problem {(A16), (B1)–(B6)} for the 1D horizontal motion of the guided point mass from initial to final phase position in the case of the (A16)-modified multiplicative quality criterion minimization where optimised value $(t_f) = ((t_f)_{16})$ of point motion final time in variable upper limit of integration in $(((x_i)^3 + u)^1{\times}(\mathrm{d}(x_i)/\mathrm{d}t)^3)$-modified minimized (A16)-functional is unknown in advance $((t_f)_{16}) = ?$ and the numerical value of $(t_f) = ((t_f)_{16}) = ((t_f)_{(J16)}) \approx 1.7\,(s)$ was estimated according to plots in Fig. 16, and where point motion time $((t_f)_{16}) \geq ((t_f)_1)$.

The obvious geometric similarity of the graphs in Figs. 1, 9, 15–18 allows us to make a completely non-obvious nonlinear-dynamic conclusion about both the variational-optimisation and the mechanical-geometric similarity of the nonlinear objective functions (A1), (A9), (A15)–(A18), written in the form of the corresponding minimized functionals.

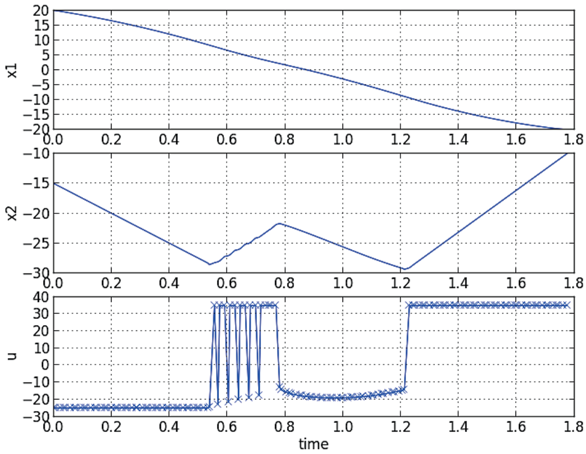

Fig. 17. Solution of the $(((x_i)^3 - u^2)^1 \times ((\mathrm{d}(x_i)/\mathrm{d}t)^3 - u^2))$-modified optimal control problem {(A17), (B1)–(B6)} for the 1D horizontal motion of the guided point mass from initial to final phase position in the case of the (A17)-modified multiplicative quality criterion minimization where optimised value $(t_f) = ((t_f)_{17})$ of point motion final time in variable upper limit of integration in $(((x_i)^3 - u^2)^1 \times ((\mathrm{d}(x_i)/\mathrm{d}t)^3 - u^2))$-modified minimized (A17)-functional is unknown in advance $((t_f)_{17}) = ?$ and the numerical value of $(t_f) = ((t_f)_{17}) = ((t_f)_{(J17)}) \approx 1.78\,(s)$ was estimated according to plots in Fig. 17, and where point motion time $((t_f)_{17}) \geq ((t_f)_1)$.

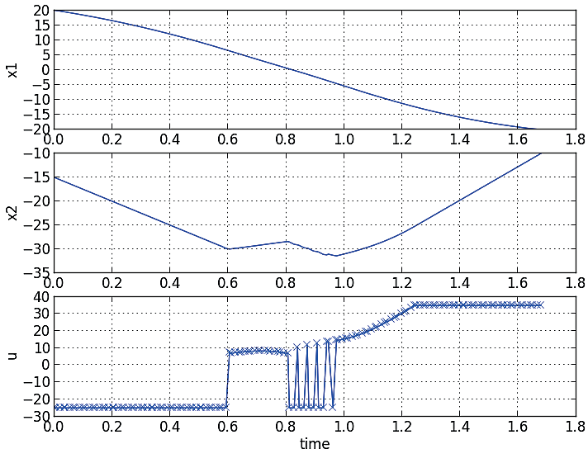

Fig. 18. Solution of the $(((x_i)^3 + u^2)^1 \times ((\mathrm{d}(x_i)/\mathrm{d}t)^3 + u^2))$-modified optimal control problem {(A18), (B1)–(B6)} for the 1D horizontal motion of the guided point mass from initial to final phase position in the case of the (A18)-modified multiplicative quality criterion minimization where optimised value $(t_f) = ((t_f)_{18})$ of point motion final time in variable upper limit of integration in $(((x_i)^3 + u^2)^1 \times ((\mathrm{d}(x_i)/\mathrm{d}t)^3 + u^2))$-modified minimized (A18)-functional is unknown in advance $((t_f)_{18}) = ?$ and the numerical value of $(t_f) = ((t_f)_{18}) = ((t_f)_{(J18)}) \approx 1.7\,(s)$ was estimated according to plots in Fig. 18, and where point motion time $((t_f)_{18}) \geq ((t_f)_1)$.

It should also be noted that there is a certain geometric similarity between Figs. 1, 4, 8, 10, 19, 20, which also “tend to reproduce” the “V”-like shape of the piecewise linear velocity graph, but with a more “floating” time scale of the movement of the controlled point compared to the final time in Fig. 1.

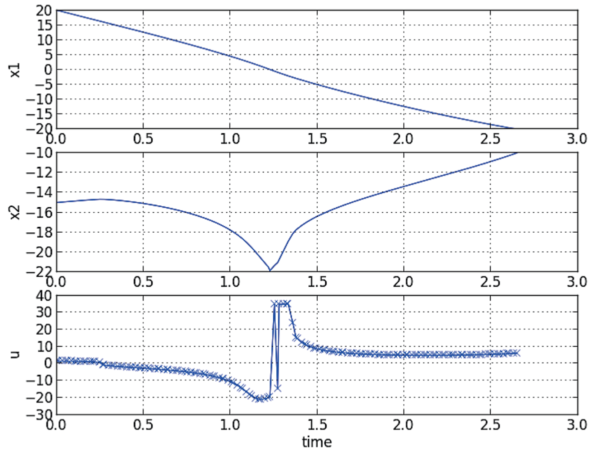

Fig. 19. Solution of the $(((x_i)^4 - u)^1 \times (\mathrm{d}(x_i)/\mathrm{d}t)^4)$-modified optimal control problem {(A19), (B1)–(B6)} for the 1D horizontal motion of the guided point mass from initial to final phase position in the case of the (A19)-modified multiplicative quality criterion minimization where optimised value $(t_f) = ((t_f)_{19})$ of point motion final time in variable upper limit of integration in $(((x_i)^4 - u)^1 \times (\mathrm{d}(x_i)/\mathrm{d}t)^4)$-modified minimized (A19)-functional is unknown in advance $((t_f)_{19}) = ?$ and the numerical value of $(t_f) = ((t_f)_{19}) = ((t_f)_{(J19)}) \approx 2.7\,(s)$ was estimated according to plots in Fig. 19, and where point motion time $((t_f)_{19}) > ((t_f)_1)$.

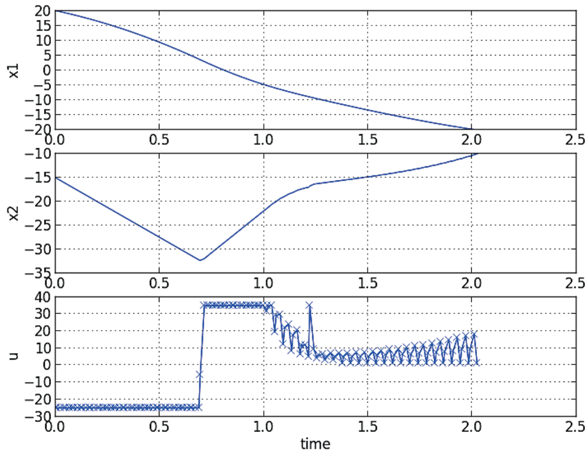

Fig. 20. Solution of the $(\exp((-1)\times x_1))\times(\sin((u-1)^2))$-modified optimal control problem {(A20), (B1)–(B6)} for the 1D horizontal motion of the guided point mass from initial to final phase position in the case of the (A20)-modified multiplicative quality criterion minimization where optimised value $(t_f) = ((t_f)_{20})$ of point motion final time in variable upper limit of integration in $(\exp((-1)\times x_1))\times(\sin((u-1)^2))$-modified minimized (A20)-functional is unknown in advance $((t_f)_{20}) = ?$ and the numerical value of $(t_f) = ((t_f)_{20}) = ((t_f)_{(J20)}) \approx 2.05\,(s)$ was estimated according to plots in Fig. 20, and where point motion time $((t_f)_{20}) > ((t_f)_1)$.

The described instructional approach proposes twenty *J*-dependent computational assignments (Figs. 1–20, [34]) for the particular states (B5) and constraints (B6), which were schematically shown in Fig. 21. The central switches of control *u*(*t*)-signal are observed in Figs. 1–3, 8–20.

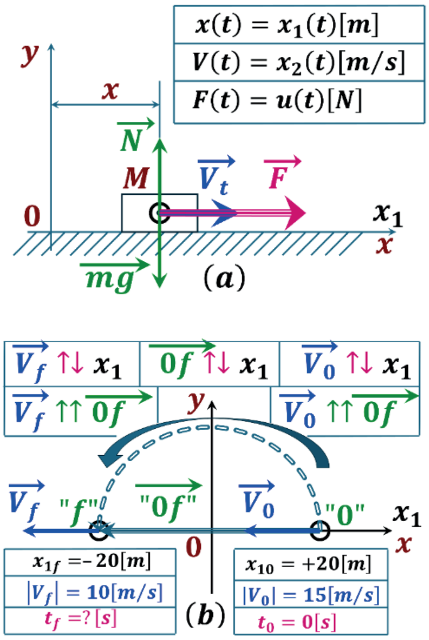

Fig. 21. Dynamic (a) and kinematic (b) schematics for *u*(*t*)-guided material particle motion from right to left (b), geometrically illustrating the numerical values of $\{x_{10}; x_{20}\}$ -states (B2), (B5) and $\{x_{1f}; x_{2f}\}$ -constraints (B3), (B6) in Table 1 for Modelica-derived computational Figs. 1–20, when the *u*(*t*)-driven point moves from right to left from the initial to the final phase position without additional stops during one-dimensional *u*(*t*)-controlled motion.

V. Discussion

Sokolov's optimisation textbook proposes rather complex structures (shapes) of minimized functionals *J* for individual student assignments at pp. 206–210 of [38]. However, Sokolov works only with upper "A"-level of controlled dynamics and completely ignores lower "B"-level of guided dynamics [38]. Therefore, Sokolov's approach provides neither plots nor any visualisation of complex shapes of Sokolov-proposed *J*-structures even for the simplest case of linear motion of a material particle. Absence of visualisations raises additional questions concerning stability and admissibility of Sokolov-proposed *J*-shapes, etc.

However, it is much more understandable and useful for engineering students to keep problem-admissible *J*-shapes of minimized functionals as simple as possible ((A1)–(A20), [34]) but to construct *J*-dependent optimisation problem completely with simultaneous mandatory assignment of both quality criterion ((A1)–(A20)) and the governing differential equations (B1) together with initial conditions (B2) & (B5), boundary conditions (B3) & (B6), and problem-related constraints on the state (phase) variables and/or control signal (B3) & (B6) (Table I and Figs. 1–21).

In contrast to Sokolov's approach [38], Perig supposes that it is much more useful to keep *J*-shapes as simple as possible but to solve *J*-dependent problem completely with Modelica freeware-derived visualisation of every particular *J*-shape on *J*-dependent plots for the phase (state) variables $\{x_1;x_2\}$ and control signal *u* in the simplest case of linear motion of material particle [34].

It is possible to expand the current twenty problems in the individual student work proposed by the author in Figs. 1–20 with sixty additional computational assignments.

In particular, the additional twenty schemes in possible Figs. 1*–20* (with one stop on the right) to the twenty considered in Figs. 1–20 (with no stops) arise through the kinematic implementation of one additional stopping point on the right in Fig. 21 through the change of the initial velocity sign from (x_{20}<0) in (B2), (B5) to (x_{20}>0), i.e., by assuming that $x_{20}^* = +15[\mathrm{m/s}]$. In this case, the above-mentioned kinematically possible Figs. 1*–20*, corresponding to the presence of an additional stop on the right, are not given in this study due to the limited volume of the manuscript. Within the framework of this mathematical formulation, we understand that the additional stopping point on the right "Stop-R" is the extreme right point in the movement of a material particle and is located to the right of the initial position "0" of the moving material point, i.e., the horizontal Cartesian coordinate of the stop on the right $\left((x_2)_{\mathrm{Stop-R}}\right)$ is greater than the horizontal Cartesian coordinate of the initial point of movement (x_{20}): $\left((x_2)_{\mathrm{Stop-R}} > x_{20}\right)$.

Another twenty calculation schemes to the forty mentioned above can be obtained in new kinematically possible Figs. 1**–20**, corresponding to the presence of one additional stop on the left, which can be algebraically specified in Fig. 21 by changing the sign of the final velocity x_{2f} of material particle from (x_{2f} < 0) in (B3), (B6) to (x_{2f} > 0), i.e., by assigning a new value $x_{2f}^{**} = +10[\mathrm{m/s}]$. Within the framework of this mathematical formulation, we understand that the additional stopping point on the left "Stop-L" is the leftmost point in the movement of a material particle and is located to the left of the final position "*f*" of the moving material point, i.e., the horizontal Cartesian coordinate of the stop on the left $\left((x_2)_{\mathrm{Stop-L}}\right)$ is less than the horizontal Cartesian coordinate of the final point of movement (x_{2f}): $\left((x_2)_{\mathrm{Stop-L}} < x_{2f}\right)$.

Twenty more kinematically admissible calculation schemes in Figs. 1***–20*** to the sixty mentioned above can be additionally formulated by simultaneously kinematically specifying both the first additional rightmost stopping point on the right "Stop-R" and the second additional leftmost stopping point on the left "Stop-L" in Fig. 21, which can be algebraically specified by simultaneously changing the initial signs of both the initial velocity of the material point (x_{20}) from minus $(x_{20} < 0)$ to plus $(x_{20} > 0)$ in (B2), (B5), i.e., by the first alternative assignment of the first new value of the initial velocity $x_{20}^* = +15[\mathrm{m/s}]$ in (B5), and the final velocity of the material point x_{2f} from minus (x_{2f} < 0) to plus (x_{2f} > 0) in (B3), (B6), i.e., by the second alternative assignment of the second new value of the final velocity $x_{2f}^{**} = +10[\mathrm{m/s}]$ in (B6).

VI. Conclusion

The paper is focused on possible Modelica-supported enhancement of guided particle dynamics curriculum both for technical mechanics and industrial optimal control courses through attracting additional student attention to more advanced and non-obvious topics of rational *J*-performance index selection techniques for the studied Newtonian dynamic system. The further impact of student chosen structure of minimized *J*-functional on Modelica-derived geometric characteristics of the targeted transient process for student-solved optimal control problem was computationally addressed in the simplest case of one-dimensional rectilinear motion of *u*-guided point mass. Twenty kinematically admissible *J*-structures of Modelica-solvable minimized *J*-functionals were proposed, formulated and comparatively $\{x_1, x_2, u\}$ visualized for linear *J*-dependent motion of a material particle with the same initial conditions, boundary conditions and two first-order differential equations of the second Newton law. Despite the relatively simple constructs of the instructor-recommended *J*-structures, the Modelica-enhanced instructional approach proposed by the author substantially broadens student understanding of *J*-performance index-dependent Newtonian dynamics for *u*-guided material particle motion.

A. Engineering and Pedagogical Advantages of the Practical Use of the Author's Computational Approach

EPA1) A practical opportunity to provide student-centric project-based learning for students of various specialties through the successful completion by each student among the target audience of a large-scale individual student assignment, either within the framework of organising a computational laboratory practical course, or within the framework of conducting a course project, or within the framework of the effective organisation of computational computer practice.

EPA2) A practical opportunity to introduce students to the constructivist approach in both engineering and engineering pedagogy. At the initial stage of their constructivist training, each student learns to construct their own dataset according to a template provided by the lecturer by carefully substituting their numbers into prepared files, then recalculating each individually prepared file using Modelica on their computer for their numbers, and then comparing the student's calculated graphs with the graphs previously calculated in the instructor's dataset. According to the author's optimistic hypothesis, at the next stage of their constructivist education, some of the students may begin to try their own hand at engineering attempts at individual student construction of both more complex differential equations with a large number of input terms with the introduction of additional numerical values of physical parameters, and in the construction of complex mathematical expressions for minimized nonlinear objective functions that provide non-obvious nonlinear dynamic trends in the optimal control of the dynamic system being studied.

EPA3) A practical engineering and pedagogical opportunity to expand the target audience's specialised understanding and demonstrate to students of various specialties the unity of conceptual, methodological, and computational methods of acausal programming, mathematical analysis, numerical analysis, general physics, mathematical physics, theoretical mechanics, analytical mechanics, variational calculus, nonlinear dynamics, cybernetics, cyberphysics, systems theory, systems analysis, model-based systems engineering, equation-based systems engineering, nonlinear optimisation, and optimal control for the effective solution of simple applied engineering problems using free software.

References

[1] J. Åkesson, K.-E. Årzén, M. Gäfvert, T. Bergdahl, and H. Tummescheit, "Modeling and optimisation with Optimica and JModelica.org – Languages and tools for solving large-scale dynamic optimisation problems", *Computers & Chemical Engineering*, vol. 34, no. 11, pp. 1737–1749, Nov. 2010. https://doi.org/10.1016/j.compchemeng.2009.11.011

[2] S. D. Bencomo, "Control learning: present and future", *Annual Reviews in Control*, vol. 28, no. 1, pp. 115–136, Jan. 2004. https://doi.org/10.1016/j.arcontrol.2003.12.002

[3] F. Biral, E. Bertolazzi, and P. Bosetti, "Notes on numerical methods for solving optimal control problems", *IEEJ Journal of Industry Applications*, vol. 5, no. 2, pp. 154–166, 2016. https://doi.org/10.1541/ieejjia.5.154

[4] J.-B. Caillau *et al.*, *OptimalControl.jl: a Julia package to model and solve optimal control problems with ODE's*. (Oct. 31, 2025). Zenodo. [Online]. Available: https://doi.org/10.5281/zenodo.17491943

[5] O. Cots and J. Gergaud, "Numerical tools for geometric optimal control and the Julia control-toolbox package", in *IVAN KUPKA LEGACY: A Tour Through Controlled Dynamics*, 1st ed. B. Bonnard, M. Chyba, D. Holcman, and E. Trélat, Eds. AIMS Sciences, 2024, pp. 209–243. [Online]. Available: https://hal.science/hal-04578955

[6] Y. A. Davizón, J. Sánchez-Leal, and E. D. Smith, "The role of optimal control theory in the curricular proposal for dynamic supply chains in industrial engineering education", *Frontiers in Education*, vol. 11, Mar. 2026, Art. no.1747320. https://doi.org/10.3389/feduc.2026.1747320

[7] J. Doyle *et al.*, "Teaching control theory in high school", in *2016 IEEE 55th Conference on Decision and Control (CDC)*, Las Vegas, USA, Dec. 2016, pp. 5925–5949. https://doi.org/10.1109/CDC.2016.7799181

[8] L. C. Evans, "Lecture notes: Version 0.2 for an old undergraduate course "An Introduction to Mathematical Optimal Control Theory". Department of Mathematics, University of California, Berkeley, Spring 2024. https://math.berkeley.edu/~evans/control.course.pdf

[9] S. Gros and M. Diehl. *Numerical Optimal Control*. Oct. 2024. [Online]. Available: https://www.syscop.de/files/2024ws/NOC/book-NOCSE.pdf

[10] K. Hauser. *Robotic Systems*. UIUC, 2024. [Online]. Available: https://motion.cs.illinois.edu/RoboticSystems/

[11] I. Horvath and G. Ábrahám, "Transdisciplinary shifts in system paradigm-driven disciplines: Mechatronics as an example", *Transdisciplinary Journal of Engineering and Science*, vol. 16, May 2025. https://doi.org/10.22545/2025/00276

[12] R. N. Jazar, "Time optimal control", in *Theory of Applied Robotics: Kinematics, Dynamics, and Control*, R. N. Jazar, Ed. Cham: Springer, 2022, pp. 731–757. https://doi.org/10.1007/978-3-030-93220-6_13

[13] U. Jönsson *et al.*, "Lectures on "Optimal control". KTH Royal Institute of Technology, February 6, 2002. [Online]. Available: https://www.user.tu-berlin.de/mtoussai/08-optimal-control/jonsson-lectureNotes.pdf

[14] S. S. Kia, "Lecture notes for the UCI course MAE 274 "Optimal Control". University of California Irvine, 2019-04-10. [Online]. Available: https://solmaz.eng.uci.edu/Teaching/MAE274/MAE274-Notes.pdf

[15] D. E. Kirk, *Optimal Control Theory: An Introduction*. New Jersey: Prentice-Hall, 1970. http://e.guigon.free.fr/rsc/book/Kirk04.pdf

[16] I. Kocsis, S Hajdu, S. Mikuska, and P. Korondi, "Introduction to the mathematics of control education in calculus for engineering students", *IEEE Transactions on Education*, vol. 68, no. 1, pp. 163–172, Feb. 2025. https://doi.org/10.1109/TE.2024.3520590

[17] J. Kong, J. Feng, Q. Zhang, T. Su, and X. Jin, "Design and practice of new engineering innovation education for automation majors", *ICCK Transactions on Education and Learning Technologies*, vol. 1, no. 1, pp. 1–13, May 2025. https://doi.org/10.62762/TELT.2025.700195

[18] R. W. Krauss, A. Ali, and A. L. Lenz, "Teaching dynamic systems and control without dynamics", in *2017 ASEE Annual Conference & Exposition*, Columbus, Ohio, USA, Jun. 2017. [Online]. Available: https://peer.asee.org/28911

[19] H. T. M. Kussaba *et al.*, "Learning optimal controllers: a dynamical motion primitive approach", *IFAC-PapersOnLine*, vol. 56, no. 2, pp. 4776–4782, Jan. 2023. https://doi.org/10.1016/j.ifacol.2023.10.1242

[20] D. Liberzon, *Calculus of Variations and Optimal Control Theory: A Concise Introduction*, Princeton, New Jersey, USA: Princeton Univ. Press, 2012. https://liberzon.csl.illinois.edu/teaching/cvoc.pdf

[21] Z. Manchester *et al.*, "Lecture Notebooks from the course 16-745 "Optimal Control and Reinforcement Learning". Carnegie Mellon University, Spring 2025. [Online]. Available: https://optimalcontrol.ri.cmu.edu/

[22] H. Maurer, "Tutorial on control and state constrained optimal control problems", SADCO Summer School 2011 – Optimal Control, Sep. 2011, London, United Kingdom. [Online]. Available: https://inria.hal.science/inria-00629518/

[23] T. Miquel, "Introduction to optimal control", CEL: Open Access Courses, Oct. 2022. [Online]. Available: https://cel.hal.science/hal-02987731v2

[24] M. R. Mojallizadeh, B. Brogliato, and C. Prieur, "Modeling and control of overhead cranes: A tutorial overview and perspectives", *Annual Reviews in Control*, vol. 56, Art. no. 100877, Jan. 2023. https://doi.org/10.1016/j.arcontrol.2023.03.002

[25] R. M. Murray, "Optimisation-based control", Version v2.3h. California Institute of Technology, Mar. 2023. [Online]. Available: https://www.cds.caltech.edu/~murray/books/AM05/pdf/obc-complete_12Mar2023.pdf

[26] B. K. Negash and N. Boizot, "Consumption minimization for a car-like robot with quadratic drag", *IFAC-PapersOnLine*, vol. 59, no. 19, pp. 638–643, Jan. 2025. https://doi.org/10.1016/j.ifacol.2025.11.107

[27] V. Nezhadali, L. Eriksson, and A. Fröberg, "Modeling and optimal control of a wheel loader in the lift-transport section of the short loading cycle", *IFAC Proceedings Volumes*, vol. 46, no. 21, pp. 195–200, Jan. 2013. https://doi.org/10.3182/20130904-4-JP-2042.00083

[28] H. Niemann, J. C. Andersen, and O. Ravn, "Towards a modern concept for teaching control engineering", *IFAC Proceedings Volumes*, vol. 42, no. 24, pp. 71–76, Jan. 2010. https://doi.org/10.3182/20091021-3-JP-2009.00015

[29] J. E. Normey-Rico and M. M. Morato, "Teaching control with basic maths: Introduction to process control course as a novel educational approach for undergraduate engineering programs", *Journal of Control, Automation and Electrical Systems*, vol. 35, no. 1, pp. 41–63, Feb. 2024. https://doi.org/10.1007/s40313-023-01063-9

[30] M. A. Pastrana *et al.*, "A novel approach to teaching theory control: Integrating STEM education, mobile robot simulation, and bio-inspired optimisation", *Operations Research Forum*, vol. 6, no. 3, Jun. 2025, Art. no. 85. https://doi.org/10.1007/s43069-025-00489-y

[31] M. Pavone *et al.*, "Lecture Notes from the course AA 203 "Optimal and Learning-Based Control". Stanford University, Spring 2024. [Online]. Available: https://stanfordasl.github.io//aa203/sp2324/

[32] A. V. Perig, A. N. Stadnik, A. A. Kostikov, and S. V. Podlesny, "Research into 2D dynamics and control of small oscillations of a cross-beam during transportation by two overhead cranes", *Shock and Vibration*, vol. 2017, 2017, Art. no.9605657. https://doi.org/10.1155/2017/9605657

[33] A. V. Perig *et al.*, "Engineering pedagogy course mapping", *Acta Metallurgica Slovaca*, vol. 28, no. 1, pp. 49–67, Mar. 2022. https://doi.org/10.36547/ams.28.1.1411

[34] O. V. Perig, "DataSet for Perig's manuscript on performance index selection teaching – ver Nov 2025", Nov. 2025, [Online]. Available: https://doi.org/10.13140/RG.2.2.29913.38245

[35] L. S. Pontryagin, *The Mathematical Theory of Optimal Processes*, 1st ed. Montreux, Switzerland: Gordon and Breach Science Publishers, 1986. https://doi.org/10.1201/9780203749319

[36] C. V. Rojas-Palacio, E. I. Arango-Zuluaga, and H. A. Botero-Castro, "Teaching control theory: A selection of methodology based on learning styles", *DYNA*, vol. 89, no. 222, pp. 9–17, Jul. 2022. https://doi.org/10.15446/dyna.v89n222.100547

[37] S. P. Sethi, *Optimal Control Theory: Applications to Management Science and Economics*. Cham: Springer Nature Switzerland, 2021. https://doi.org/10.1007/978-3-030-91745-6

[38] S. V. Sokolov, *Optymalni ta adaptyvni systemy* [*Optimal and adaptive systems*]. Sumy: Sumy State University, 2018. [Online]. Available: http://essuir.sumdu.edu.ua/handle/123456789/68042 [in Ukrainian].

[39] O. A. Stenin *et al.*, *Optymalni systemy upravlinnia* [*Optimal control systems*]. Kyiv: NTUU KPI (National Technical University of Ukraine). Available: https://library.kpi.kharkov.ua/uk/math_physics_Optsiu [in Ukrainian].

[40] J. Tar *et al.*, "Abstraction in teaching ways of control engineering to support the understanding of mathematics behind Industry 4.0 – a Hungarian approach", *IFAC-PapersOnLine*, vol. 55, no. 17, pp. 230–235, Jan. 2022. https://doi.org/10.1016/j.ifacol.2022.09.284

[41] R. Tedrake, "Underactuated robotics: Algorithms for walking, running, swimming, flying, and manipulation", (Course Notes for MIT 6.832). [Online]. Available: https://underactuated.csail.mit.edu/

[42] K. L. Teo, B. Li, C. Yu, and V. Rehbock, *Applied and Computational Optimal Control: A Control Parametrization Approach*. Cham: Springer Nature Switzerland, 2022. https://doi.org/10.1007/978-3-030-69913-0

[43] T. Vámos, B. Ruth, L. Keviczky, and D. Sík, "Methodology of teaching the first control course", *Opus et Educatio*, vol. 7, no. 2, Jan. 2020. https://doi.org/10.3311/ope.375

[44] R. Weber, "Lecture notes for the course "Optimisation and Control". University of Cambridge, Lent Term 2016. [Online]. Available: https://www.dpmms.cam.ac.uk/~rrw1/oc/index.html

[45] D. Wu *et al.*, "Graduate course "Optimal Control 2023". Department of Automatic Control, Lund University, Lund, Sweden, 2023. [Online]. Available: https://www.control.lth.se/education/doctorate-program/optimal-control/optimal-control-2023/

[46] Z. Yang, "Operation control of visualization VR teaching platform for mechanical manufacturing professional course under iterative learning PID algorithm", *Discover Computing*, vol. 29, no. 1, Jan. 2026, Art. no. 22. https://doi.org/10.1007/s10791-025-09879-6

[47] K. Zenger, "Control engineering, system theory and mathematics: the teacher's challenge", *European Journal of Engineering Education*, vol. 32, no. 6, pp. 687–694, Dec. 2007. https://doi.org/10.1080/03043790701520719

Oleksandr Viktorovych Perig was born in 1980 in the city of Sloviansk. He graduated from the Faculty of Physics and Mathematics of the Sloviansk State Pedagogical Institute in 2002 and received a specialist diploma in the specialty "Pedagogy and Methodology of Secondary Education. Physics". In 2011, in the city of Kramatorsk, he defended his diploma of Candidate of Technical Sciences in the specialty 05.03.05 "Processes and machines for pressure treatment" at the Donbas State Engineering Academy (DSEA). In 2014, in the city of Kramatorsk, he received the academic title of Associate Professor of the Department of Automation of Industrial Processes of the DSEA. His main area of current research is related to the social and dynamic problems of engineering education (EE) and engineering psychology with current didactic emphases on the methodological foundations of mechanical EE, electrical EE, control EE, and network EE.

Since 2002, he has been working as an instructor at DSEA, where from September 2002 to May 2012, he worked as an Assistant Lecturer at the Department of Technical Mechanics at DSEA; from June 2012, he worked as a Senior Lecturer at the Department of Technical Mechanics at DSEA; from January 2013, he worked as a Senior Lecturer at the Department of Automation of Industrial Processes, and since May 2013, he has been working as an Associate Professor at the Department of Automation of Industrial Processes at DSEA. His current research interests focus on automation-cybernetic modelling of nonlinear engineering and pedagogical processes of teaching and learning in complex socio-technical systems. During his career, he has written 115 journal reviews verified by the Web of Science.

E-mail: Oleksandr.Perih@ddma.edu.ua
ORCID iD: https://orcid.org/0000-0002-6923-6797